# Characterization of Aerogel Prepared High-Surface-Area Alumina: In Situ FTIR Study of Dehydroxylation and Pyridine Adsorption

**Abbas A. Khaleel[b] and Kenneth J. Klabunde*[a]**

**Abstract:** Mesoporous high-surface-area alumina was prepared by a modified aerogel procedure. Specific surface areas between 530-685 $m^2 g^{-1}$ were obtained after heat treatment at 500 °C. Nitrogen adsorption studies have shown that surface areas and pore characteristics change upon decomposition of aluminum hydroxide to oxide as well as upon compaction of oxide powders. The surface area of aluminum hydroxide increased to a maximum, while the pore volume and diameter decreased as the hydroxide was heated to a temperature of 400 °C. Heating at higher temperatures resulted in sintering of the particles accompanied by a decline in the surface area. Compaction of activated alumina into pellets was accompanied by a relatively gradual change in the surface area and pore characteristics at pressures below $6.9 \times 10^7$ Pa, while severe changes took place at a pressure of $1.4 \times 10^8$ Pa. In situ IR studies of the dehydroxylation of the alumina surface, showed ν(OH) absorptions for isolated surface hydroxy groups centering at 3670, 3714, and 3765 $cm^{-1}$, which are shifted to lower frequencies than common literature values. Pyridine was found to adsorb on $Al^{3+}$ ions as well as through hydrogen bonding to relatively acidic surface OH groups, and IR spectra indicated the presence of strong Lewis acid sites.

**Keywords:** adsorption · aerogels · alumina · mesoporous materials · nanotechnology

## Introduction

The synthesis and applications of nanoscale materials have triggered a great deal of interest in recent years.[1–5] Their importance stems from the unusual behavior they have shown compared with their bulk counterparts with respect to chemical and physical properties. Of special interest to chemists is the high surface area of metal oxides and their chemical properties, especially their remarkable potential as heterogeneous catalysts as well as sorbents.

Alumina powder has been widely studied and employed as a catalyst as well as a support for other catalytic materials such as metals and metal oxides,[6–9] and is commercially available in surface areas between 150—250 $m^2 g^{-1}$, while higher surface area materials have been obtained from sol–gel preparations.[10–14]

The surface composition of alumina has been widely studied because of its important role in catalytic processes. Both IR,[15–18] $^1H$ and[27] Al NMR spectroscopy[19, 20] have been employed as powerful tools to study the surface composition of these materials. Coordinatively unsaturated $Al^{3+}$ ions and surface hydroxy (OH) groups are believed to play a key role in the catalytic behavior of high surface area alumina, and various structural models have been proposed.[21–23]. Owing to the presence of tetrahedrally ($T_d$) and octahedrally ($O_h$) coordinated $Al^{3+}$ sites on the surface, several stretching vibrational frequencies for surface hydroxy groups have been observed in the FTIR spectrum of alumina. Structures and FTIR assignments of these groups will be discussed in more detail herein.

Alumina is known to possess an acidic surface, and the nature and the degree of acidity has been widely studied[18, 22] by adsorbing probe molecules such as ammonia,[24] carbon monoxide,[18] and pyridine.[25] While pyridine is relatively a strong base, it is weaker than ammonia and is preferred in some cases due to the fact that it may not react with some of the weaker sites that would react with ammonia. One of the objectives of the current study was to investigate whether very high surface area alumina exhibits any differences in its behavior, including its interaction with pyridine, over known lower surface area alumina.[25] FTIR spectroscopy has proven to be a good tool for studying the adsorption of pyridine since it allows investigation of the changes in the pyridine ring vibrations in the 1400–1700 $cm^{-1}$ region of the spectrum.

Herein, we report our results from a recent study of high-surface-area alumina. We have studied the process of trans-

[a] Prof. K. J. Klabunde
Department of Chemistry
Kansas State University
Manhattan, KS 66506 (USA)
Fax: (+1) 785 532-6666
E-mail: kenjk@ksu.edu

[b] Prof. A. A. Khaleel
Department of Chemistry
United Arab Emirates University
P.O. Box 17551, Al-Ain (UAE)

  0947-6539/02/0817-3991 $ 20.00+.50/0 

forming a high-surface-area hydroxide aerogel into ultrafine alumina powder, dehydroxylation of alumina samples at different temperatures, effect of compaction on the surface area and porosity, and finally the adsorption of pyridine as a probe molecule to ascertain the surface acidity.

It should be noted that other authors have also described high surface area alumina samples prepared by sol–gel methods.[10–14] Some differences between these previous results and the present work are: In the current work, 1) no organic additives have been used; 2) hydrolysis and gelation were carried out at room temperature; 3) two different starting materials and several different solvents have been compared; 4) higher surface areas were achieved.

## Results and Discussion

**Preparation and characterization of high-surface-area alumina:** The two alkoxide precursors employed in this study resulted in mesoporous aluminum hydroxide aerogels with specific surface areas (SSA) between 500–800 $m^2g^{-1}$ and average pore diameters (APD) between 90–130 Å. Upon heat treatment at 500 °C under dynamic vacuum, the hydroxide was converted to highly divided aluminum oxide with a SSA in the range between 530–685 $m^2g^{-1}$ and an average pore diameter of between 70–100 Å.

Table 1 shows some characteristics measured for the as-prepared aluminum hydroxide aerogel before and after activation (conversion to alumina) at 500 °C versus some preparational variables, specifically, the type of precursor and the solvents used.

Table 1. Some characteristics of aluminum hydroxide before and after thermal dehydration to alumina at 500 °C.[a] Data in parentheses corresponds to the alumina.

| Precursor | Solvent[b] | SSA [$m^2g^{-1}$] | TPV[c] [$cm^3g^{-1}$] | APD[d] [Å] | Density [$gcm^{-3}$] |
|---|---|---|---|---|---|
| Al-tri-isopropoxide | alcohol | 755 (680) | 2.20 (1.35) | 125.5 (84.5) | 2.45 (2.58) |
| | mixture | 663 (590) | 2.09 (1.42) | 132.3 (97.1) | 2.59 (2.64) |
| Al-tri-*sec*-butoxide | alcohol | 621 (559) | 2.30 (1.41) | 98.1 (98.0) | 2.62 (2.65) |
| | mixture | 559 (570) | 1.76 (1.24) | 94.7 (87.0) | 2.60 (2.63) |

[a] Data presented in this table are taken from representative experiments and data reproducibility within 10 % was obtained. [b] Alcohol refers to the corresponding alcohol, and mixture refers to the same alcohol mixed with toluene. [c] TPV = total pore volume. [d] APD = average pore diameter.

As shown in Table 1, the surface area of alumina obtained from aluminum tri-isopropoxide was always higher than that obtained from *sec*-butoxide. In part, this could be due to the solvent used in each case. *sec*-Butyl alcohol has a critical temperature of 263 °C as compared to 235 °C for 2-propanol. Since in both cases the temperature of drying the gel in the autocalve was 265 °C, more complete removal of the solvent in the case of isopropoxide is expected. Also the final pressure in the autoclave obtained when the solvent was 2-propanol was higher than that obtained from *sec*-butyl alcohol. Higher pressure during the heating stage may aid in limiting the aggregation of particles, and hence better protects the pores in the material.

Two solvent systems were used: the corresponding alcohol, 2-propanol or *sec*-butyl alcohol, or a mixture of the alcohol and toluene. The presence of toluene gives a very clear gel while in the case of alcohol alone the solubility of alkoxide was lower (more time was needed to dissolve it), and an opaque gel was obtained upon hydrolysis. We have observed the following differences in the final products obtained from both systems. First, the apparent density of the hydroxide aerogel obtained from toluene-containing systems was always about two–three times higher than that obtained from alcohol-alone systems. When toluene is not present in the solvent, finer and more fluffy-looking powder was obtained as compared to chunky-looking product in the case where toluene was present. Second, the surface area was about 10–15 % higher, in most of our trials, when toluene was not involved. Third, the color of the alumina after activation at 500 °C was generally slightly darker when the toluene/alcohol mixture was used, indicating more carbonacious deposits. Again, we think that these effects are due to the difference in the critical temperature of the solvents. While 2-propanol and *sec*-butyl alcohol have critical temperatures of 235 and 260 °C, respectively, toluene has a critical temperature of 315 °C. The temperature of the supercritical drying treatment, employed in this study, was 265 °C which leads to higher pressure and more complete removal of the solvents in the case of alcohol alone, especially for 2-propanol due to its lower critical temperature.

Densities measured for the hydroxide aerogel samples were in the range between 2.2–2.6 g $cm^{-3}$; however, they increased slightly (2.4–2.7 $gcm^{-3}$) upon activation at 500 °C. For comparison, the density for commercial high surface are alumina (from Aldrich, SSA = 155 $m^2g^{-1}$) was measured by the same technique showing a density of 3.16 $gcm^{-3}$. Particle sizes of between 3 and 4 nm for the hydroxide and the oxide samples were calculated based on the SSA and density measurements. A corresponding estimated particle size was also obtained for alumina activated to 500 °C from the TEM image shown in Figure 1. Powder XRD studies showed very broad patterns, typical of amorphous materials, which did not allow us to assign the alumina phase type or calculate the crystallite size.

The $N_2$ adsorption/desorption isotherms obtained for both hydroxide and oxide samples were all typical H3 type and in very few cases H2 type (IUPAC classification), which in both cases represents mesoporous materials with mixed-pore systems (Figure 2). Figure 2 shows also the BJH analyses for pore volume distribution. In the case of the hydroxide, the BJH analyses show a broader distribution of the pore volume and a larger portion of large pores than for alumina.

**Surface area and porosity at different activation temperatures**: Portions from a hydroxide sample were activated at different temperatures for four hours. For each sample, the SSA, the porosity, and density were measured after the heat treatment. Results for the different temperatures are shown in Table 2.

The surface area of the aerogel hydroxide increases as it is heated under dynamic vacuum at temperatures below 400 °C. This indicates that at temperatures below 400 °C, the hydrox-

  0947-6539/02/0817-3992 $ 20.00+.50/0 *Chem. Eur. J.* **2002**, *8*, No. 17

Figure 1. TEM image of an alumina sample activated at 500 °C.

Table 2. Specific surface area and porosity of alumina as a function of heat treatment temperature.

| Temperature [°C] | SSA [$m^2 g^{-1}$] | TPV [$cm^3 g^{-1}$] | APD [Å] |
|---|---|---|---|
| hydroxide | 530 | 2.20 | 100.0 |
| 250 | 641 | 1.34 | 83.7 |
| 300 | 649 | 1.40 | 85.2 |
| 400 | 587 | 1.24 | 84.5 |
| 500 | 575 | 1.25 | 87.2 |
| 700 | 422 | 1.21 | 88.9 |

ide aerogel undergoes decomposition where each particle fragments into a number of particles resulting in higher specific surface areas. As they are heated at higher temperatures, above 400 °C, they tend to sinter producing larger particles and lower SSA. The overlap between the two processes, activation (decomposition) and sintering, gives rise to a maximum in the curve of surface area versus heat treatment temperature at about 400 °C as indicated in Table 2.

While the specific surface area increased upon activation to temperatures below 400 °C, the TPV and the average pore

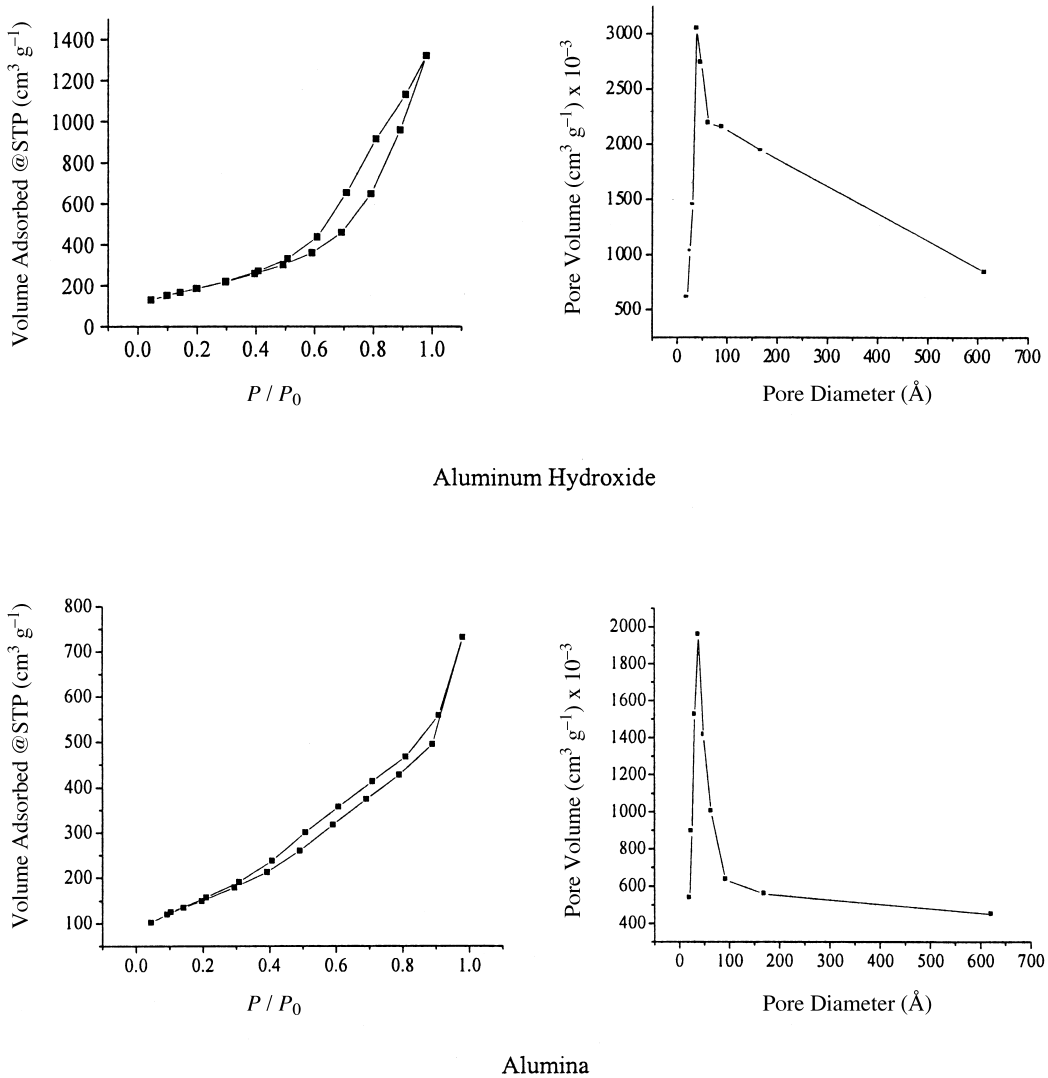


Figure 2. $N_2$ adsorption/desorption isotherms (left) and BJH pore volume distribution profiles (right) of aluminum hydroxide and aluminum oxide (alumina) samples.

  0947-6539/02/0817-3993 $ 20.00+.50/0 

diameter (APD) decreased from the beginning of the process, at 250 °C. At temperatures above 250 °C, the TPV and APD seem to be stable. From this behavior, it is likely that the hydroxide loses a significant portion of it large pores as a result of fragmenting into smaller particles, which results in an increase in the SSA. After this decomposition process is complete and a full conversion to oxide is achieved, most of the large pores are already lost and the TPV and the APD become relatively stable. On the other hand, the particles tend to sinter into larger particles (at temperatures higher than 400 °C) such that the SSA decreases without noticeable change in the porosity. This behavior is clearly indicated from the BJH pore volume distribution profiles in Figure 2, where the activated alumina profile shows a sharper distribution with a much lower predominance of large pores than observed for the hydroxide.

**Surface area and porosity versus compaction (pelletizing) pressure**: Portions of an alumina sample (pre-activated at 500 °C) were pelletized at different pressures by using a hydraulic press. Samples were then ground, and a $N_2$ adsorption study was carried out on each. Results of BET, SSA, and porosity measurement are presented in Table 3.

Table 3. SSA and pores' characteristics of alumina pellets versus pressure of compaction.

| | Powder | Pellets, pressure of compaction [Pounds] | | |
|---|---|---|---|---|
| | | 5000 | 10000 | 20000 |
| surface area [$m^2 g^{-1}$] | 558 | 508 | 486 | 311 |
| total pore volume [$cm^3 g^{-1}$] | 2.19 | 0.87 | 0.59 | 0.26 |
| average pore diameter [Å] | 132.4 | 74.3 | 52.6 | 33.2 |

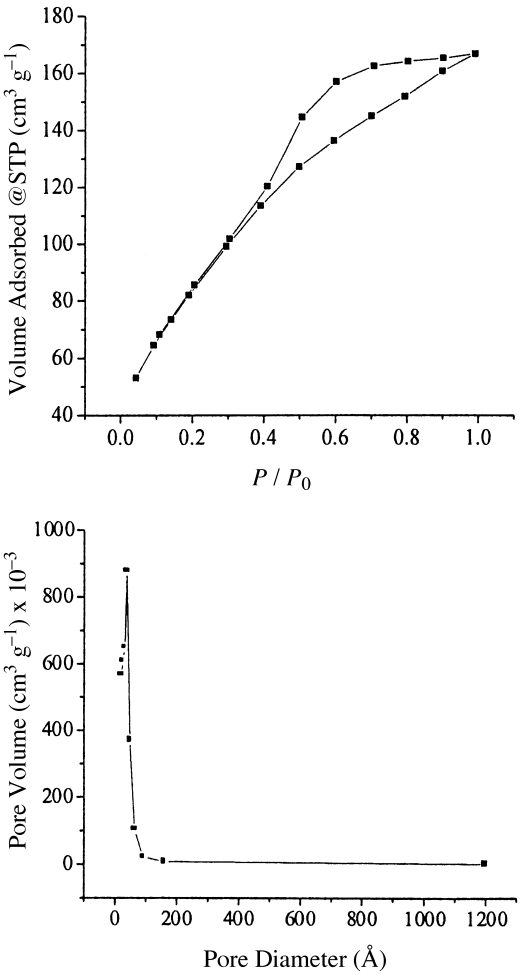


Figure 3. $N_2$ adsorption/desorption isotherm and BJH pore volume distribution for alumina pellets compacted at 20000 pounds.

While the surface area decreased gradually and slightly upon compaction below $3.4 \times 10^8$ Pa, the TPV and APD decreased more significantly. This indicates that the compaction below this pressure has resulted in significant shrinkage of large pores without a significant increase in primary crystallite sintering. At very high pressure, $6.9 \times 10^8$ Pa, severe loss of pore volume and considerable sintering takes place, resulting in a considerable loss in the SSA and porosity. The $N_2$ adsorption/desorption isotherm and BJH analysis presented in Figure 3 shows clearly this effect. The isotherm shown, deviates significantly from the typical isotherms of mesoporous materials shown in Figure 2, showing no considerable capillary condensation behavior but mainly adsorption on a microporous-like material. The BJH pore volume distribution shows a very sharp maximum centered at a diameter of about 30 Å, and a lack of large pores.

**In situ IR study of dehydroxylation of aluminum hydroxide/oxide**: An important and interesting region of the spectrum is the ν(OH) region that shows the transformation of the hydroxide to oxide and the residual surface hydroxy species as the sample is heated. The spectrum of the as-prepared hydroxyl aerogel shows a very broad absorption band between 3200 $cm^{-1}$ and 3770 $cm^{-1}$ which is a typical feature for hydrogen-bonded, network-like or associated, hydroxy groups. Upon heating, the broad band below 3600 $cm^{-1}$ disappears gradually and is almost eliminated at 500 °C. This absorption corresponds to the molecularly adsorbed water and associated OH groups. At temperatures above 500 °C, only strongly bound, isolated or non hydrogen-bonded, hydroxy groups remain attached to the surface and show absorption bands between 3670 and 3775 $cm^{-1}$. Absorptions at 3670 and about 3750 $cm^{-1}$ were removed more favorably as a significant decrease in their intensities was observed at temperatures above 400 °C.

Similar IR absorption bands have been observed by others and have been associated with structurally different aluminum sites on the surface.[21–23] On the surface of alumina particles, two coordinatively different types of aluminum ions are encountered, tetrahedral ($T_d$) and octahedral ($O_h$), which have coordination numbers of four and six, respectively. Based on these two different coordinations of aluminum ions on the surface, five types of hydroxy groups have been proposed to be present on the surface of alumina.[22] The structures of these types are shown in Figure 4 along with their observed absorption frequencies as proposed by Knözinger and Ratnasamy.[22] The occurrence of each type differs from one sample to another depending on the planes exposed.



0947-6539/02/0817-3994 $ 20.00+.50/0 *Chem. Eur. J.* **2002**, *8*, No. 17

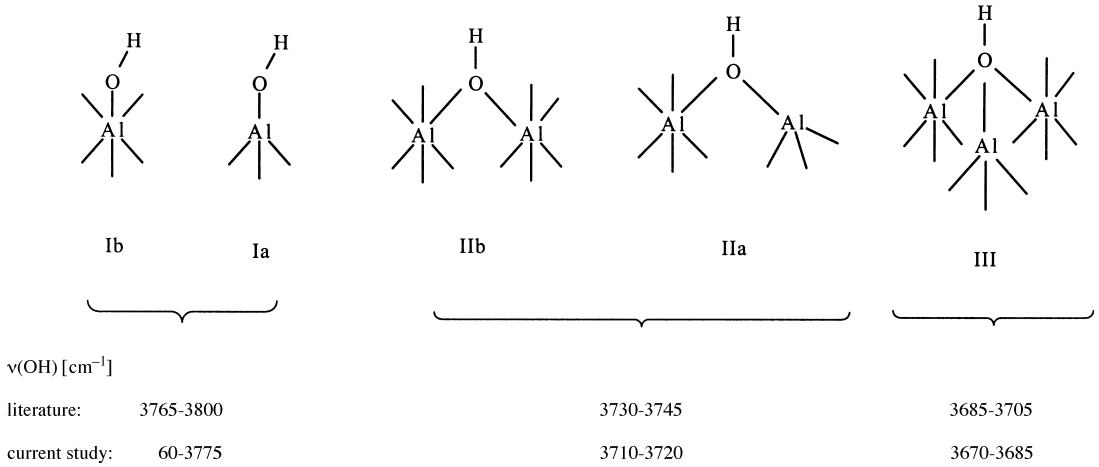


Figure 4. Proposed structures of different surface hydroxyl groups on alumina.

However; based on structural considerations, the bridging-type species occur more frequently.

Accordingly, five ν(OH) peaks are expected in the IR spectrum. In the literature,[15] these five absorptions have been observed to occur at three main frequencies, 3695, 3735, and 3795 cm$^{-1}$ for alumina with specific surface area, 100–300 m$^2$ g$^{-1}$. In some cases they were resolved into the following five absorptions: 3695–3705, 3730–3735, 3740–3745, 3760–3780, and 3785–3800.[22]

For the high-surface-area alumina, in this study, we have observed similar IR spectra, but, interestingly, we have found that these bands shift significantly to lower frequencies. As shown in Figure 5, these bands center at 3675, 3714, and 3765 cm$^{-1}$, involving a shift of 15–25 wavenumber units.

Comparing the dehydroxylation process of our samples with those reported in the literature,[15, 22] we find a good correspondence in the intensities and behavior of the absorption bands upon heat treatment. As an example, the bands at 3700 and 3765 were reported to more readily decrease in intensity compared to others, which corresponds to what we have observed for absorptions at 3675 and about 3750 cm$^{-1}$ in our spectra. Significant decrease in the intensity of these two absorption bands is shown at 400 °C, which indicates that these two absorptions are due to relatively easily removable hydroxy groups, and are very likely to be associated with the most basic Ia group and the most acidic III group (Figure 4). This fact allows us to propose that absorptions in our spectra are due to hydroxy groups that are structurally similar to those proposed in Figure 4. Thus, dehydroxylation is believed to be more favored when basic and acidic hydroxy groups are present next to each other allowing elimination of water molecules. At later stages of dehydroxylation, after such groups are removed, a considerable migration of surface OH species is required to facilitate their removal, as water molecules, which takes place only at higher temperatures.

It is possible that the frequency shifts we observe are due to higher Brønsted acidity of the OH groups in question. This, in turn, indicates that the oxygen atom of the hydroxy groups on our samples binds more strongly to the surface than it does on lower surface area samples. These observations suggest that

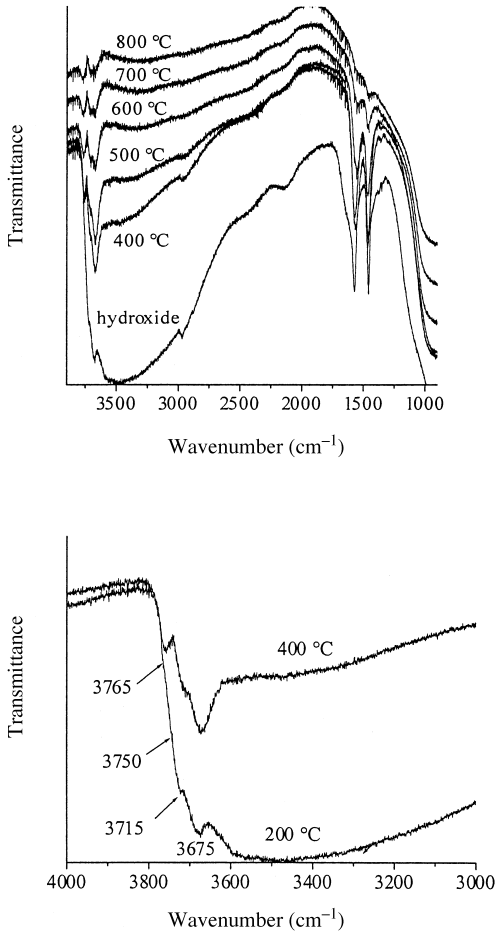


Figure 5. FTIR spectra of aluminum hydroxide/oxide at different activation temperatures.

the very high-surface-area alumina, in this study, shows stronger Lewis acidity associated with the $Al^{3+}$ sites than observed for reported lower surface area alumina. This could be due to the fact that high surface areas led to a higher concentration and a higher degree of coordination unsaturation for surface sites. Such surfaces should exhibit stronger Lewis acidity and are expected to show a high degree of reactivity as well.

**Adsorption of pyridine:** Pyridine, as a good Lewis base, adsorbs on alumina surfaces through interaction with two types of acidic sites, Brønsted acid hydroxy (OH) sites and Lewis $Al^{3+}$ sites. As a result, three types of adsorbed pyridine species can be observed (Figure 6). a) Coordinately adsorbed

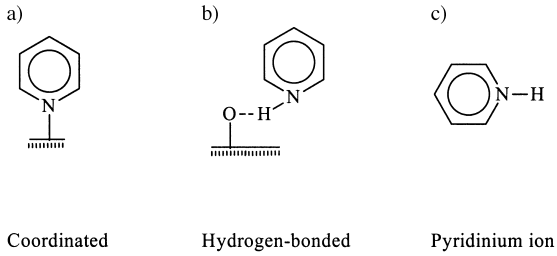


Figure 6. Different pyridine adsorption modes. a) ccordinated, b) hydrogen-bonded, c) pyridinium ion.

pyridine, which results from interaction between a surface Lewis acid site ($Al^{3+}$) and the pyridine molecule through its lone pair on the nitrogen atom. The amount and the binding strength directly correlates with the amount and the Lewis acidity of such surface sites. b) Hydrogen-bonded pyridine, which results from hydrogen bonding between relatively acidic hydroxy groups and pyridine nitrogen atom. c) Pyridinium ion, which results from the abstraction of a proton from a Brønsted acid hydroxy group.

For the pyridinium ion and hydrogen-bonded pyridine, the $N^+-H$ stretching vibration would be of interest, but due to hydrogen bonding, its absorption is usually considerably broadened and difficult to detect. Figure 7 shows the IR spectra of an alumina sample before adsorption, after

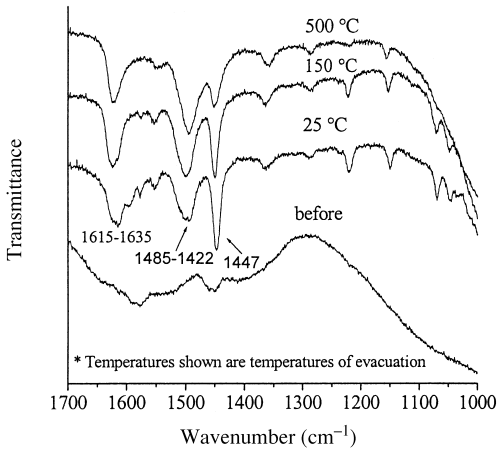


Figure 7. FTIR spectra of adsorbed pyridine on alumina. Spectra of the solid before and after adsorption and spectra after desorption at different temperatures.

adsorption at room temperature, as well as after desorption at different temperatures. The spectrum for adsorption at room temperature does not show significant peaks for free or physically adsorbed pyridine which are typically at about 1440 and 1583 $cm^{-1}$,[25] indicating that nearly all of the pyridine is chemisorbed. (A very weak peak at about 1583 $cm^{-1}$ that is eliminated upon desorption at 150 °C indicates that only an insignificant amount of pyridine was physically adsorbed.) Strong absorptions at 1447, 1485–1500, and 1610–1635 indicate a considerable adsorption through coordination to Lewis acid sites. The presence of the pyridinium ion would be indicated by a strong absorption band at about 1540 $cm.^{-1}$.[25] The absence of such a peak shows that no pyridinium ion species exist. On the other hand, hydrogen-bonded pyridine exhibits absorptions around 1440–1447 (very strong), 1485–1490 (weak), 1580–1600 (strong) $cm^{-1}$, which in our spectra exist but overlap with those for coordinated pyridine. Assigning these peaks was aided by studies reported on IR spectra of a series of pyridine complexes involving coordinated as well as hydrogen-bonded pyridine.[26] Two pieces of evidence support the presence of hydrogen-bonded pyridine. First, upon desorption at 500 °C, the absorption band at about 1447 $cm^{-1}$ decreases significantly in intensity without accompanied similar loss in the other bands. The fact that hydrogen-bonded pyridine exhibits absorption in this region very strongly, supports the fact that this intensity decrease is due to removal of hydrogen-bonded pyridine. The intensity decrease at 1447 $cm^{-1}$ was also accompanied by removal of the shoulder at about 1485 $cm^{-1}$ and the weak band at about 1595 $cm^{-1}$ which are also assigned for hydrogen-bonded pyridine. In contrast, an overlapping band at 1455 does not decrease, and this we believe is because the 1455 band is due to very strong coordination of pyridine to Lewis acid sites. Second, as the adsorption of pyridine proceeds, the ν(OH) absorptions disappear, as a result of considerable broadening. Upon desorption at 500 °C and the removal of hydrogen-bonded pyridine, they partially reappear, indicating their significant involvement and interaction with pyridine.

Going back to the ring stretching vibration region, adsorption of pyridine on acidic surfaces is always accompanied by a shift in its absorption bands to higher frequencies. It has been observed that the degree of this shift correlates with the Lewis acidity of the adsorption sites.[25] As a result, the degree of this shift is considered as an indicator of the surface Lewis acidity. As an example, when pyridine is adsorbed on MgO,[27] the 1583 $cm^{-1}$ band does not show any shift, while for the relatively acidic silica[28] surface it shifts to 1620 $cm^{-1}$. On the alumina in this study, this absorption shifts to about 1630–1635 $cm^{-1}$.

Current and previous observations indicate that, as the strength of pyridine binding to the surface increases, the higher frequency shift of the absorptions increases.[25, 26, 28] As shown in Figure 7, upon evacuation at 500 °C, the absorption bands narrow with an intensity decrease on their low frequency side. This may indicate the presence of different Lewis acid sites that vary in their acidity. Pyridine that adsorbs at the relatively weaker sites desorb first. One may expect such results from highly divided powders whose surfaces deviate considerably from perfection with a high and varying degree of coordination unsaturation of surface sites.

The stability of coordinately bound pyridine after evacuation at 500 °C and the considerable shift of the 1583 $cm^{-1}$ band to 1630–1635 $cm^{-1}$ demonstrate the strong Lewis acidity of our high-surface-area $Al_2O_3$ samples. Besides the strong Lewis acidity behavior, this alumina exhibits some increased Brønsted acidity through the surface hydroxy groups.



0947-6539/02/0817-3996 $ 20.00+.50/0 *Chem. Eur. J.* **2002**, *8*, No. 17

## Conclusion

Mesoporous high-surface-area alumina was obtained through an aerogel preparation using alkoxide precursors. We found that the preparation procedure is sensitive to several variables such as the type of alkoxide precursor, the type of solvent(s) used, the temperature of the supercritical drying, and the heat treatment procedure. $N_2$ adsorption studies have shown that surface areas and pore characteristics change upon decomposition of aluminum hydroxide to oxide. The surface area of aluminum hydroxide increased to a maximum, while the pore volume and diameters decreased significantly as the hydroxide was activated to a temperature of 400 °C. Heating at higher temperatures resulted in sintering of the particles accompanied by a decrease in the surface area. Compaction of activated alumina into pellets was accompanied by a relatively small decrease in the surface area and a more significant decrease in the pore volume and diameters at pressures below $6.9 \times 10^7$ Pa, while severe changes to the surface area and the pores took place at a pressure of $1.4 \times 10^8$ Pa. In situ IR studies of the dehydroxylation of the alumina surface showed ν(OH) absorptions for isolated surface hydroxy groups centering at 3675, 3714, and 3765 $cm^{-1}$. These absorption bands are shifted to lower frequencies (15–25 $cm^{-1}$ difference) than for known literature values. We attribute this difference to the stronger Lewis acidity of the $Al^{3+}$ sites on the surface, which leads to stronger Al–OH bonds and hence weaker O–H bonds. Pyridine adsorption studies also indicated the strong Lewis acidity of the $Al^{3+}$ sites and the relatively significant Brønsted acidity of the surface hydroxy groups by showing strongly hydrogen-bonded pyridine.

## Experimental Section

**Synthesis and characterization of high-surface-area alumina**: High-surface-area $Al_2O_3$ was synthesized through a modified aerogel procedure using aluminum triisopropoxide or aluminum tri-*sec*-butoxide as precursors. In a typical experiment, aluminum triisopropoxide (3.0 g, 0.0147 mol) was dissolved in 2-proanol (130 mL) and toluene (170 mL), or in 2-propanol (300 mL). While the solution was stirred, water (0.80 mL, 0.0444 mol) (dissolved in 2-propanol (15 mL)) was added dropwise. A clear gel (opaque in the absence of toluene) formed and was stirred for 14 h. In a typical experiment using aluminum tri-*sec*-butoxide, the same procedure was followed by using the precursor (15 mL) in *sec*-butyl alcohol (200 mL) and 250 mL toluene or in 450 mL *sec*-butyl alcohol and was hydrolyzed with water (1.20 g, 0.0666 mol) dissolved in *sec*-butyl alcohol (15 mL). The gel was dried under near supercritical conditions by using an autoclave reactor. Starting with a $7 \times 10^5$ Pa nitrogen pressure the reactor was heated to 265 °C at a rate of 1.0 K $min^{-1}$ and the final pressure was in the range of 6–$9 \times 10^6$ Pa. This pressure (nitrogen plus solvent vapor) was released quickly. A white ultrafine powder of aluminum hydroxide aerogel was obtained, which was converted to alumina by heating under dynamic vacuum at 500 °C for 4 h. The heat treatment is a very sensitive process and affects some characteristics of the final product. As an example, when the temperature was raised quickly to the final level of 500 °C, more carbonaceous deposits, indicated from a darker color, were obtained. This could be due to fact that the allowed time was not enough for solvent–residual removal, resulting in more high-temperature decomposition of the remaining solvent. Better samples were obtained when the temperature was raised to 500 °C gradually. It was raised at increments of 50 K and held at each temperature for 15 min, except at 350 °C where it was held for one hour. From the pressure change during activation, it is indicated that most of the dehydration takes place between 340–380 °C. Results as a function of different preparational variables are summarized in Table 1.

Alumina samples were studied by powder X-ray diffraction (XRD), transmission electron microscopy (TEM), and $N_2$ adsorption for BET surface area and porosity structure.

**In situ IR study of the dehydroxilation process of aluminum hydroxide/oxide:** Samples for this study were prepared as self-supported thin films pressed, using a hydraulic press, on a tungsten grid. The tungsten grid was mounted, through nickel clamps, in a special cell in which the sample can be heated to different temperatures, as high as 1000 °C. The cell is linked directly to an ultra high vacuum line (ca. $1 \times 10^{-6}$ Torr) where in situ IR spectra could be recorded. The cell design is described in detail in reference [29].

**Adsorption of pyridine**: Pyridine adsorption was studied on alumina samples by IR spectroscopy. The same apparatus and sample preparation described above for the in situ IR system were employed. The sample was heated at 500 °C for two hours and cooled to room temperature under vacuum. Pyridine was then introduced to the sample at a pressure of 5.0 Torr and the IR spectrum was recorded after two hours where the pressure in the cell dropped to about one Torr.

The desorption process of adsorbed pyridine was also studied by evacuating and heating the sample at different temperatures. At each desorption temperature the cell was evacuated for one hour (ca. $1 \times 10^{-4}$ Torr) then cooled to room temperature before an IR spectrum was recorded.

**Chemicals and instrumentation:** All chemicals used in this study were purchased from Aldrich and stored under nitrogen. BET surface areas and porosity were estimated by using nitrogen adsorption at 77 K on a Quantachrome NOVA-1200 instrument. Density measurements were carried out using gas pycnometry on a Quantachrome Multipicnometer 1000 instrument, where ultra high pure helium was employed. Estimated particle sizes were measured from TEM images and were also calculated by using the following equation which relates the specific surface area of a sphere particle with its diameter: $D = 6/\delta S$, where $D$ is the particle diameter, $\delta$ is its density, and $S$ is the specific surface area.[30] TEM images were obtained using a Philips 201 electron microscope. XRD analysis were carried out on a Scintag XDS 2000 diffractometer using a $Cu_{K\alpha}$ radiation source. Diffraction data was collected in the $2\theta$ angle range of 20–85°.

All IR studies were carried out on an ATI Mattson Research 1 Series spectrophotometer equipped with a liquid nitrogen cooled MCT detector with a resolution of 0.5 $cm^{-1}$. The instrument was checked for reliability by recording the standard spectrum of a polystyrene film.

## Acknowledgements

The support of the National Science Foundation is acknowledged with gratitude.

[1] *Nanophase Materials: Synthesis, Properties, Applications* (Eds.: G. C. Hadjipanayis, R. W. Siegel), Kluwer, London, **1994**.
[2] K. J. Klabunde, C. Mohs in *Chemistry of Advanced Materials: An Overview* (Eds.: L. Interrante, M. Hampden-Smith), Wiley-VCH, New York, **1998**, pp. 271–327.
[3] A. Khaleel, K. J. Klabunde, D. Park, *High Temp. Mater. Sci*. **1995**, *33*, 99.
[4] E. Lucas, S. Decker, A. Khaleel, A. Seitz, S. Fultz, A. Ponce, W. Li, C. Carnes, K. J. Klabunde, *Chem. Eur. J.* **2001**, *7*, 2505.
[5] K. J. Klabunde, *Nanostructured Materials in Chemistry*, Wiley, New York, **2001**.
[6] H. Knözinger, *Adv. Catal*. **1976**, *25*, 184.
[7] Y. Mizushima, M. Hori, *Appl. Catal. A* **1992**, *88*, 137.
[8] C. N. Satterfield, *Heterogeneous Catalysis in Practice*, McGraw-Hill, New York, **1980**, Section 4.5.
[9] A. Khaleel, P. Kapoor, K. J. Klabunde, *Nanostruct. Mater*. **1999**, *11*, 459.
[10] N. D. Parkyns, *J. Catal*. **1972**, *27*, 34–44.
[11] Y. Mizushima, M. Hori, *J. Non-Crystalline Solids* **1994**, *170*, 215.

  0947-6539/02/0817-3997 $ 20.00+.50/0 

[12] K. Tadanaga, H. Kobayashi, T. Minami, *J. Non-Crystalline Solids* **1998**, *225*, 230.
[13] E. Elaloui, A. C. Pierre, G. M. Pajonk, *J. Catal*. **1997**, *166*, 340.
[14] C. Pierre, F. Elaloui, G. M. Pajonk, *Langmuir* **1998**, *14*, 66.
[15] A. A. Tsyganenko, V. N. Filimonov, *J. Mol. Struct*. **1973**, *19*, 579.
[16] J. A. Lercher, H. Noller, *J. Catal*. **1982**, *77*, 152.
[17] J. C. Lavalley, M. Benaissa in *Adsorption and Catalysis on Oxide Surfaces* (Eds.: M. Che, G. C. Bond), Elsevier, Amsterdam, **1985**.
[18] T. H. Ballinger, J. T. Yates, *Langmuir*, **1991**, *7*, 12, 3041.
[19] J. J. Fitzgerald, G. Piedra, S. F. Dec, M. Seger, G. E. Maciel, *J. Am. Chem. Soc*. **1997**, *119*, 7832.
[20] G. W. Wagner, L. R. Procell, R. J. O′cner, S. Munavalli, C. Carnes, P. Kapoor, K. J.Klabunde, *J. Am. Chem. Soc*. **2001**, *123*, 1636.
[21] J. B. Peri, *J. Phys. Chem*. **1965**, *69*, 220.
[22] H. Knözinger, P. Ratnasami, *Catal. Rev.-Sci. Eng*. **1978**, *17*(1), 31.
[23] K. Sohlberg, S. J. Pennycook, S. T. Pantelides, *J. Am. Chem. Soc*. **1999**, *121*, 10999.
[24] R. T. Barth, E. V. Ballou, *Anal. Chem*. **1961**, *33*, 1081.
[25] E. P. Parry, *J. Catal*. **1963**, *2*, 371.
[26] N. S. Gill, R. H. Nuttal, D. E. Scaife, D. W. A. Sharp, *J. Inorg. Nucl. Chem*. **1961**, *18*, 79.
[27] H. Itoh, S. Utamapanya, J. Stark, K. J. Klabunde, J. R. Schlup, *Chem. Mater*. **1993**, *5*, 71.
[28] B. A. Morrow, I. A. Cody, *J. Phys. Chem.* **1976**, *80*, 1995.
[29] J. T. Yates, Jr., *Experimental Innovations in Surface Science*, Springler, New York, **1998**.
[30] R. S. Mikhail, E. Robens, *Microstructure and Thermal Analysis of Solid Surfaces*, Wiley, New York, **1983**.

Received: November 6, 2001
Revised: May 23, 2002 [F3662]

  0947-6539/02/0817-3998 $ 20.00+.50/0 